ISSN 1063-7826, Semiconductors, 2012, Vol. 46, No. 7, pp. 901–912. © Pleiades Publishing, Ltd., 2012.
Original Russian Text © M.M. Mezdrogina, M.V. Eremenko, E.I. Terukov, Yu.V. Kozhanova, 2012, published in Fizika i Tekhnika Poluprovodnikov, 2012, Vol. 46, No. 7, pp. 925–936.

SURFACES, INTERFACES, AND THIN FILMS

Intensity of Emission from Intracenter 4*f*-Transitions in *a*-Si:H, ZnO, and GaN Films Doped with Rare-Earth Ions

M. M. Mezdrogina[a]^, M. V. Eremenko[a], E. I. Terukov[a], Yu. V. Kozhanova[b]

[a] *Ioffe Physical–Technical Institute, Russian Academy of Sciences, St. Petersburg, 194021 Russia*

^ *e-mail: margaret.m@mail.ioffe.ru*

[b] *St. Petersburg State Polytechnic University, St. Petersburg, 195251 Russia*

Submitted December 28, 2011; accepted for publication January 13, 2012

Abstract—It is shown that the intensity of emission from intracenter 4*f*-transitions in amorphous *a*-Si:H films and crystalline (GaN, ZnO) films doped with rare-earth ions is governed by the local environment of doping impurity ions. In the case of *a*-Si:H, a pseudo-octahedron with the C_{4V} point group is present due to nanocrystallites, which provides a local environment for rare-earth ions. In the case of a hexagonal crystal lattice in crystalline GaN and ZnO films, the local symmetry of rare-earth ions introduced into the semiconductor matrix by diffusion, with a pseudo-octahedron with the C_{4V} point group, is formed by stresses due to rare-earth ion–oxygen complexes with a radius exceeding that of host ions incorporated at crystal lattice sites. In contrast to GaN films, ZnO films exhibit, on being doped with Tm, Sm, and Yb, both high-intensity emission in the long-wavelength spectral region, characteristic of intracenter 4*f* transitions in rare-earth ions, and a substantial increase in intensity in the short-wavelength spectral region ($\lambda = 368$–370 nm). GaN films doped with rare-earth ions exhibit in this spectral range only an inhomogeneously broadened emission spectrum due to the presence of an emission band characteristic of donor-acceptor recombination.

DOI: 10.1134/S1063782612070135

1. INTRODUCTION

Doping of wide-gap semiconductors with rare-earth metals is extensively studied in order to create new optoelectronic devices. Rare-earth ions (REIs) in a semiconductor matrix are not only an object of study, but also a researcher's tool, an optical probe that makes it possible to determine the parameters of a semiconductor. The most extensively studied REI impurities in semiconductors are Er and Eu because Er has an intracenter 4*f* transition $^4I_{13/2}$–$^4I_{15/2}$ ($\lambda =$ 1540 nm), and Eu, a transition $^5D_1$–$^7F_1$ ($\lambda = 623$ nm). Extensive studies of Eu-doped wide-gap direct-gap crystalline GaN (GaN:Eu) have led to the observation of lasing and the development of light-emitting diodes (LEDs) for the wavelength $\lambda = 622$ nm, necessary for creating white LEDs [1, 2].

Another wide-gap semiconductor ZnO [3] with the free-exciton binding energy $E = 60$ meV is a promising material for lasing to be observed at room temperature. Doping of ZnO films with Eu impurity by using Y_2O_3:Eu:ZnO enabled observation of the lasing effect [4], and the introduction of three REIs led to the development of a white LED [5].

Most studies concerned with the potential for raising the intensity of emission due to the intracenter 4*f* transition in Er, $^4I_{13/2}$–$^4I_{15/2}$ ($\lambda = 1540$ nm) in films of amorphous hydrogenated silicon *a*-Si:H doped with Er [*a*-Si:(H, Er)] have been carried out because of the prospects for use of this semiconductor in fiber-optic communication systems [6], owing to the possibility of its integration into silicon technology.

To elucidate the mechanism by which REI luminescence spectra are formed in ZnO, GaN, and *a*-Si:H, it is necessary to analyze (i) the position of REIs in the semiconductor matrix and the interaction of REIs with defects and impurities, (ii) position of the energy levels of REIs relative to the valence and conduction bands of the semiconductors, (iii) excitation mechanisms and kinetic models describing the luminescence related to intracenter 4*f* states in REIs, (iv) REI luminescence quenching processes, and (v) the influence exerted by the concentration of REIs and an additionally introduced impurity (co-dopant), introduced into the semiconductor, on its photoluminescence (PL) spectra.

Several studies on *a*-Si:(H, Er) have been devoted to solving a number of problems mentioned above [6–8]. In [6, 7], basic results obtained when analyzing the influence exerted by the local environment of REIs in the amorphous matrix of *a*-Si:H were reported. These results are used in studies of crystalline semiconductor matrices, GaN:(Eu, Er) and ZnO:(Eu, Er).

The goal of our study was to examine the possibility of raising the intensity of the emission due to intracenter 4*f* transitions in Er and Eu in amorphous (*a*-Si:H) and crystalline (ZnO, GaN) films.

2. EXPERIMENTAL

The *a*-Si:H films were grown by magnetron and high-frequency sputtering. The dopants (metallic and gaseous) were introduced during the course of film growth.

Single-crystal ZnO films were produced by the ac magnetron sputtering of a ZnO target, with metallic dopants introduced by diffusion, and gas impurities (nitrogen) introduced by high-frequency annealing of the films in an argon–nitrogen mixture.

Wurtzite GaN crystals were grown by the metal-organic chemical vapor deposition (MOCVD) decomposition of metal-organic mixtures, with metallic dopants introduced by diffusion.

The concentrations of the metallic impurities in the undoped films under study was determined by X-ray fluorescence analysis using an XP1-Apt installation at the temperature $T = 300$ K. The X-ray diffraction analysis of the ZnO films was performed at a URS-69 installation.

The optical measurements of PL spectra were carried out using an SDL-2 diffraction spectrometer with an inverse linear dispersion of 1.3 nm mm^{-1} and a spectral resolution (slits) of 2.6 Å in the spectral regions of edge- and impurity-type luminescence of the amorphous and crystalline films under study.

Several types of lasers served as sources of radiation for PL excitation in the steady-state mode.

(I) A continuous-wave (CW) He–Cd laser with the emission wavelength $\lambda = 325$ nm and emission power 15 mW (band-to-band excitation of GaN, ZnO).

(II) A CW argon-ion laser of the LG-106M type with an emission power of 0.5 W and emission wavelength selection with a rotated prism mounted in place of the 100% mirror, which enabled lasing at a wavelength of $\lambda = 488$ nm (band-to-band excitation of *a*-Si:H) and excitation of intracenter transitions in rare-earth ions.

(III) Pulsed nitrogen laser of the LGI-21 type with a pulse width $\tau = 7$ ns at half-maximum, repetition frequency of 100 Hz, average power of 3 mW, and an emission wavelength of $\lambda = 3371$ Å. The power density of the pulse in a defocused beam was ~10 kW cm^{-2}.

To enable correct comparison of the emission spectra of various films (*a*-Si:H, GaN, ZnO), the parameters being controlled (beam incidence angle, excitation light intensity, temperature) were maintained constant. The PL spectra of the *a*-Si:(H, Er) films were measured at $T = 77$ and 300 K, and those of GaN and ZnO, at $T = 15$ and 77 K.

The charge state of the REIs was identified by Mössbauer spectroscopy, with the Mössbauer isotope ^{169}Tm for Er, and ^{151}Eu for Eu.

In the case of *a*-Si:H films, Mössbauer sources were produced by irradiation of the films with thermal neutrons at a fluence of 5×10^{18} cm^{-2}. Capture of a thermal neutron, ^{168}Er(n, γ)–^{169}Er, and the subsequent β decay of ^{169}Er yields ^{169}Tm Mössbauer probes at Er sites. The Mossbauer spectra of ^{169}Tm were measured at $T = 295$ K, with thulium ethyl sulfate as the absorber.

The metallic impurity Eu contains the Mössbauer isotope ^{151}Eu. In this case, the role of the absorber was played by $^{151}Sm_2O_3$; $T = 295$ K.

3. EXPERIMENTAL RESULTS AND DISCUSSION

Our combined measurements of the PL spectra, REI concentrations, and charge state of the Er impurity demonstrated that Er–O clusters are emitting centers in *a*-Si:(H, Er) films and the local symmetry of Er^{3+} ions is similar to the symmetry in Er_2O_3. It was shown that the size of clusters formed by [Er_2O_3] complexes strongly affects the PL intensity during exciton energy transfer from the *a*-Si:H matrix to Er ions. The role of oxides [Si–O], i.e., the concentration of oxygen, consists in the formation of the optimal concentration and dimensions of [Si–O] complexes.

The data furnished by Mössbauer emission spectroscopy on the ^{169}Er(^{169}Tm) isotope demonstrated that Er_2O_3 clusters are photoluminescent centers. It was also shown that, as the content of the Er impurity is raised to 1.08%, with a simultaneously increasing O concentration, the emission intensity of the intracenter 4*f* transition in Er ($^4I_{13/2}$–$^4I_{15/2}$, $\lambda = 1540$ nm) increases. Further increase in the concentration of the impurities leads to a decrease in the emission intensity for the transition with $\lambda = 1540$ nm. Figure 1 shows how the concentration of the Er impurity affects the type of microstructure of the *a*-Si:(H, Er) films. At Er contents as high as 1.08%, the presence of a crystalline phase is indicated by the microdiffraction pattern. It is shown that the interplanar spacings in the diffraction pattern correspond to those in the compound Er_2O_3. Microstructural analysis was used to determine the crystallite size (from 5 to 50 nm) and the particle density (5×10^{10} cm^{-2}). Lowering the Er content to 0.79% leads to an increase in the crystallite size to 50–250 nm, with the particle density decreasing to 5×10^9 cm^{-2}. The film changes its structure, it becomes cellular, and the new phase crystallized in these cells reproduces their shape. The microdiffraction pattern of this film also shows reflections from Er_2O_3. As the Er content is lowered further to 0.34%, porosity appears in the film.

Figure 2 shows how the content of the Er impurity affects the emission intensity of the band at $\lambda = 1540$ nm. It can be seen that changes in the crystallite size and film structure (see Fig. 1) correlate with changes in the PL spectra: a decrease in the size of nanocrystallites leads not only to an increase in the PL

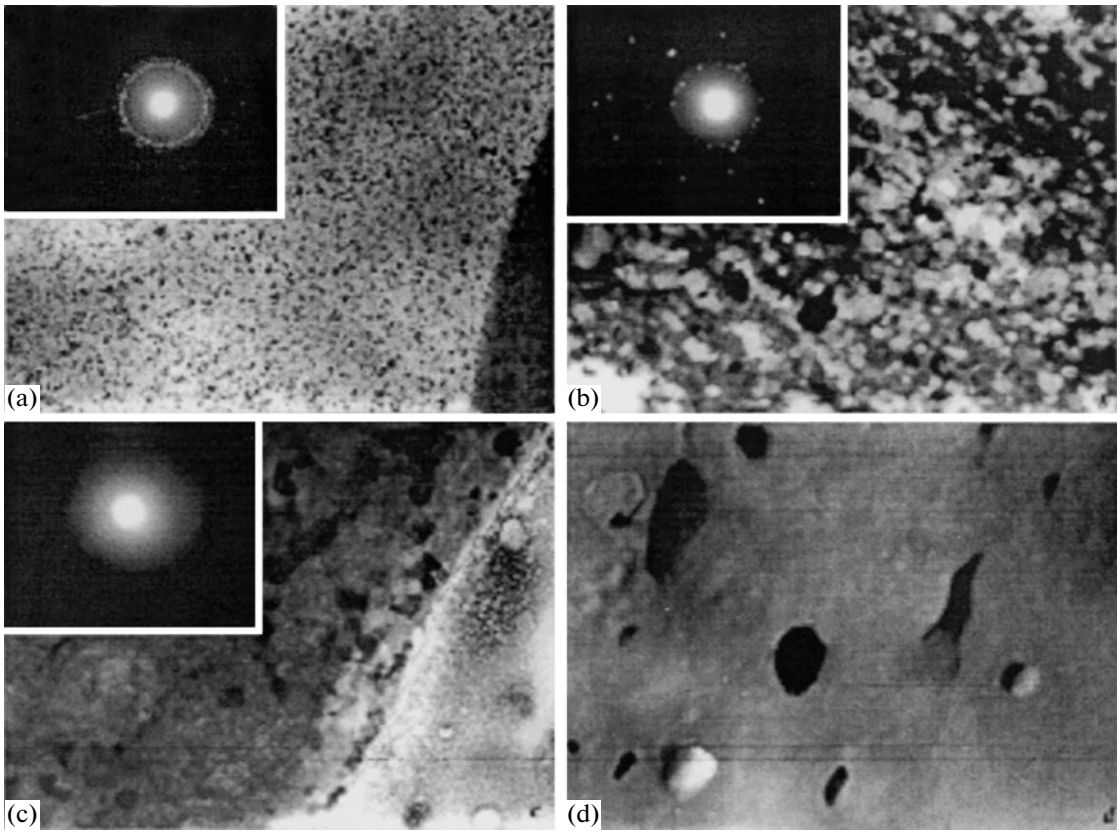

Fig. 1. Microstructure of *a*-Si:(H, Er) films with erbium contents C_{Er} of (a) 1.08, (b) 0.79, and (c, d) 0.34%. Insets: microdiffraction patterns.

intensity, but also to a shift of the emission peak to shorter wavelengths. If we consider the nearest environment of Er^{3+} ions, [Er^{3+} + O] complexes have a lower symmetry than the six-coordinated [Er^{3+} + Si]. [Er^{3+} + O] are weakly bound to the disordered structural network of *a*-Si:H because of the existence of a strong internal bond [6]. Self-organization processes (the formation of nanocrystals in the amorphous matrix) lead to an increase in the emission intensity of the band at $\lambda = 1540$ nm and to its weak temperature quenching. The presence of nanocrystals is a necessary condition for excitation energy transfer to Er ions because the excitation energy is transferred from excitons in Er_2O_3 nanocrystallites to the Er ion, with accompanying radiative recombination, which results in an intracenter 4*f* transition in Er with $\lambda = 1540$ nm.

To enable injection pumping, it is necessary to solve the complicated technological problem of optimizing the dopant (Er and O) concentrations.

We studied the effect of Eu (Mössbauer spectra were measured for ^{151}Eu) on the PL spectra of amorphous *a*-Si:(H, Eu) films. Depending on the film deposition mode (the substrate temperature), the Mössbauer spectrum had the form of superimposed lines of Eu^{3+} (lower intensity) and Eu^{2+} (higher intensity) at the maximum deposition temperature $T_S = 380°C$. Lowering the deposition temperature to $T_S = 280°C$ resulted in the appearance of only Eu^{2+} centers in the spectrum. Electrical measurements demonstrated that the introduction of a Eu impurity shifts the emission peak to longer wavelengths, but no high-intensity emission due to intracenter 4*f* transitions in Eu^{3+} ($\lambda =$ 622 nm) was observed [9].

At present, the mechanisms by which Er and Eu emission spectra are formed in GaN wurtzite crystals and InGaN/GaN quantum-well (QW) structures are the most intensively studied. It has been shown that REIs in GaN are isovalent impurities substituting Ga in the crystal lattice. In this case, trigonal centers are formed in which three bonds are equivalent (with lengths of 2.21, 2.14, and 2.15 Å for Eu^{3+}, Er^{3+}, and Tm^{3+}, respectively) and one is directed along the *c* axis of GaN and has a length shorter by ~0.03 Å. These lengths coincide to within 3% with extended X-ray absorption fine structure (EXAFS) data [10]. It was also found that the Ga–N bond length (1.95 Å) differs from the Er–N bond length (2.14 Å), which indicates that there are stresses in the crystal lattice. At the same time, it has been shown that compressive stresses are present in undoped GaN samples [11]. Consequently, it can be concluded that crystal stresses are compen-

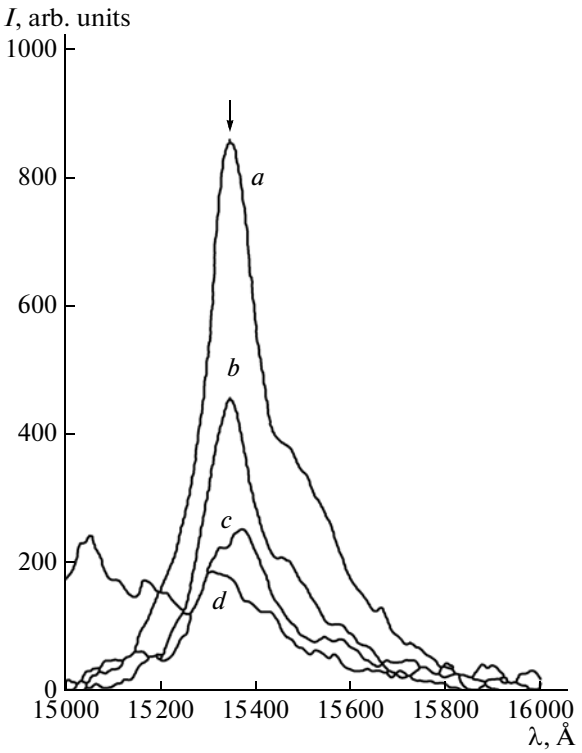

Fig. 2. PL intensity for *a*-Si:(H, Er) films with erbium contents C_{Er} of (*a*) 1.08, (*b*) 0.79, and (*c*, *d*) 0.34%.

sated to a certain extent upon the introduction of REIs into the GaN semiconductor matrix. When crystalline GaN films are doped with REIs, the bonding type changes from covalent-ionic (Ga–N) to ionic (Er–N) [10]. REIs were introduced into the GaN matrix both during crystal growth (MOCVD, MBE) and by implantation and diffusion [10, 11]; the REI concentration was widely varied to determine the optimal concentration and the optimal position of the impurity ion in the crystal lattice in order to obtain the maximum emission intensity of intracenter 4*f* transitions. It has been shown that the maximum intensity of intracenter transitions is observed if the position of REIs is close to that of electrically active (*n*-type) structural defects in GaN [12].

Emission Mössbauer spectroscopy was used to determine the charge state of Eu both in GaN films and in InGaN/GaN QW structures at varied concentrations of impurity–defect complexes in the structures under study. If the doping Eu ion in the crystalline GaN matrix is in a single-charge state, emission due to the intracenter 4*f* transition in Eu^{3+} is observed with $\lambda = 622$ nm. If there are two charge states, Eu^{3+} and Eu^{2+}, no emission band is observed at $\lambda = 622$ nm and defect gettering by REIs occurs. At the same time, if the Eu impurity ion is in the Eu^{2+} charge state, magnetic ordering is observed upon application of a magnetic field and hysteresis loops appear.

The mechanism of energy transfer from the GaN semiconductor matrix to REIs was considered in [13]. Four main types of excitation transfer can be distinguished for wide-gap materials.

The first type of excitation transfer is observed when REIs form a complex defect that gives rise to a donor level in the energy gap of the semiconductor. The role of this defect can be played by $RE_{Ga} + V_N$ [14]. In this case, an electron can be captured to the donor level of a complex defect with the participation of a REI and recombine with a hole at an acceptor level, related to the presence of some foreign impurity. The recombination energy can be transferred by an Auger process to the inner 4*f* shells of REIs. This energy transfer mechanism is of a resonant nature. A slight mismatch between the energy of the excited state of a REI and the donor–acceptor recombination (D–A) energy is possible since an energy excess (deficiency) can be compensated for by the generation (absorption) of several (1–3) optical phonons [15]. However, as with any resonant process, it can occur in both directions, which will lead to quenching of the REI-related luminescence. Therefore, a slight excess in the (D–A) recombination energy over the excited-state energy at low temperatures can play a positive role in the suppression of quenching processes.

The second type of processes is important if a REI forms a complex with other defects or impurities, which gives rise to an acceptor level in the energy gap, e.g., a $RE_{Ga} + V_{Ga}$ complex [15]. In this case, an Auger process of energy transfer to the 4*f* states of a REI during/upon the recombination of an electron at a foreign donor and a hole at an acceptor level of a complex defect incorporating a REI.

The third mechanism is associated with energy transfer during/upon the recombination of an electron and a hole that are bound to an impurity donor and an impurity acceptor. The efficiency of all three mechanisms described above must, in all probability, strongly depend on the distance between the recombining hole and electron, i.e., on the distance between the corresponding impurities in the crystal. This is so since there is a Coulomb interaction between the electron and hole, which depends on the distance r as $1/r^2$. Hence it can be concluded that the larger the distance, the lower their binding energy and the smaller the probability of their recombination followed by energy transfer to REIs. If the third mechanism is in operation, the distance between the donor and acceptor impurities and a rare-earth ion also becomes important. As this distance increases, the probability of Auger energy transfer must, in all probability, decrease.

Finally, the fourth type of excitation mechanisms consists of energy transfer from a free exciton to an REI (which is important at low temperatures) and energy transfer during/upon the recombination of an electron from a deep level in the valence band.

All these processes are resonant, but resonance conditions alone are insufficient for effective energy transfer to the intracenter states of REIs. It is also necessary to ensure the low probability of reverse energy transfer processes. This can be attained, in particular, by correct choice of the carrier lifetimes at the donor and acceptor impurity levels involved in the energy transfer processes. This situation is in part similar to the case of three- and four-level laser schemes in which there are long- and short-lived states between which lasing occurs and there are no energy absorption processes. The aforesaid gives a key to understanding the effect of co-doping (the introduction of additional impurities) with REIs in semiconductor matrices.

The intensity of emission due to intracenter 4*f* transitions in REIs in a semiconductor matrix is known to be inversely proportional to the defect concentration in this matrix, all other conditions being the same. In *n*-GaN films deposited by chloride-hydride vapor phase epitaxy (HVPE), 10^{18} cm^{-3} < $N_d - N_a$ < 10^{19} cm^{-3} [16], doping with Eu led only to defect gettering and no emission characteristic of intracenter transitions in Eu^{3+} was observed. In MOCVD-grown REI-doped *n*-GaN with 10^{17} cm^{-3} < $N_d - N_a$ < 10^{18} cm^{-3}, emission due to intracenter transitions in REIs was observed. The spectra of intracenter transitions in Sm, Eu, Er, and Tm are shown in Fig. 3. It can be seen that the intensities of emission due to intracenter 4*f* transitions in REIs are different at the same concentrations of impurities or defects in the GaN matrix: the intensity in the case of Sm and Tm exceeds that for Eu and Er. It has been shown that the Er impurity tends to undergo segregation [17]. Introduction of additional impurities O, Eu, Zn [18] leads to an increase in the intensity of emission due to intracenter 4*f* transitions. It should also be noted that, as a rule, the films mentioned above exhibit an emission band at $\lambda = 520$–540 nm, which indicates that there is a shallow donor and a deep acceptor center because of the presence of a $V_{Ga}O_N$ defect, where V_{Ga} is a Ga vacancy and O_N is oxygen in place of N. If the concentration of these defects is high, the intensity of emission due to intracenter 4*f* transitions in REIs will be low [19], i.e., the optimal concentration of defects in the semiconductor matrix is necessary. According to the results of electron-microscopy (Figs. 4a, 4b) and atomic force microscopy (AFM) studies (Figs. 4c, 4d), the microstructure of GaN films doped with REIs and an additionally introduced impurity includes clusters [19]. Figures 4c and 4d show the surface morphology of GaN:(Mg + ER + Zn); the emission spectrum is presented in Fig. 3c.

In structures with GaN/InGaN QWs, all the above four excitation mechanisms remain important. However, the presence of QWs can be regarded as an additional source of carriers with energies determined by the heterostructure's design. This makes possible a fifth type of energy transfer to REIs, with the involvement of carriers from the well. Since the luminescence spectrum of intracenter 4*f* transitions is unique to each rare-earth ion and strongly depends on its local environment, we may assume that QWs with different sizes and compositions are necessary for excitation of different REIs.

The main quenching mechanisms of excited intracenter 4*f* states of rare-earth ions in GaN single crystals and heterostructures based on this semiconductor can be divided into four types.

The first of these is associated with nonradiative Auger recombination processes, which can occur when a REI with excited intracenter 4*f* states interacts with an electron bound to another REI trap (a complex made up of a REI and a defect/background impurity) [15]. The following two processes involve a REI trap with excited intracenter states and an electron (hole) at a neutral donor (acceptor) [20]. An important role is played by Auger quenching involving free carriers in wide-gap semiconductors at high temperatures and under laser excitation [20]. In GaN/InGaN QW heterostructures, quenching is also possible in an interaction of REIs with excited intracenter states and 2D carriers localized in the QWs.

The second type of mechanisms by which excited states of localized centers in semiconductors nonradiatively recombine is multiphonon relaxation [21]. As demonstrated by numerous studies, the most critical parameter affecting the multiphonon emission rate is the energy gap to the nearest lower-lying level. If this gap is sufficiently wide, the probability of multiphonon processes is negligible as compared with radiative processes.

The third and fourth types of mechanisms are the resonant migration of excitation to a certain impurity, including another REI [22], and cross-relaxation between two REIs [23, 24]. These mechanisms are responsible, together with nonradiative Auger recombination, for the so-called "concentration" quenching of REI-related luminescence in the GaN semiconductor matrix and heterostructures based on this material.

Also important, together with the structural features of REIs in a semiconductor matrix, the mechanism of energy transfer to intracenter states of the REIs, and REI luminescence quenching, is the influence exerted by the concentration of REIs introduced into a semiconductor on the luminescence spectrum, considered above for the example of *a*-Si:(H, Er). An important experimental fact in the doping of GaN with an REI impurity (Eu) is the dependence of the relative intensities of three emission peaks ($\lambda = 618$–624 nm) on the Eu concentration. These intensities vary greatly with the Eu content (from 2 to 3.5%) and remain virtually unchanged at concentrations in the range 4% < [Eu] < 1%. This behavior is due, in the opinion of the authors of [23, 24], to a structural phase

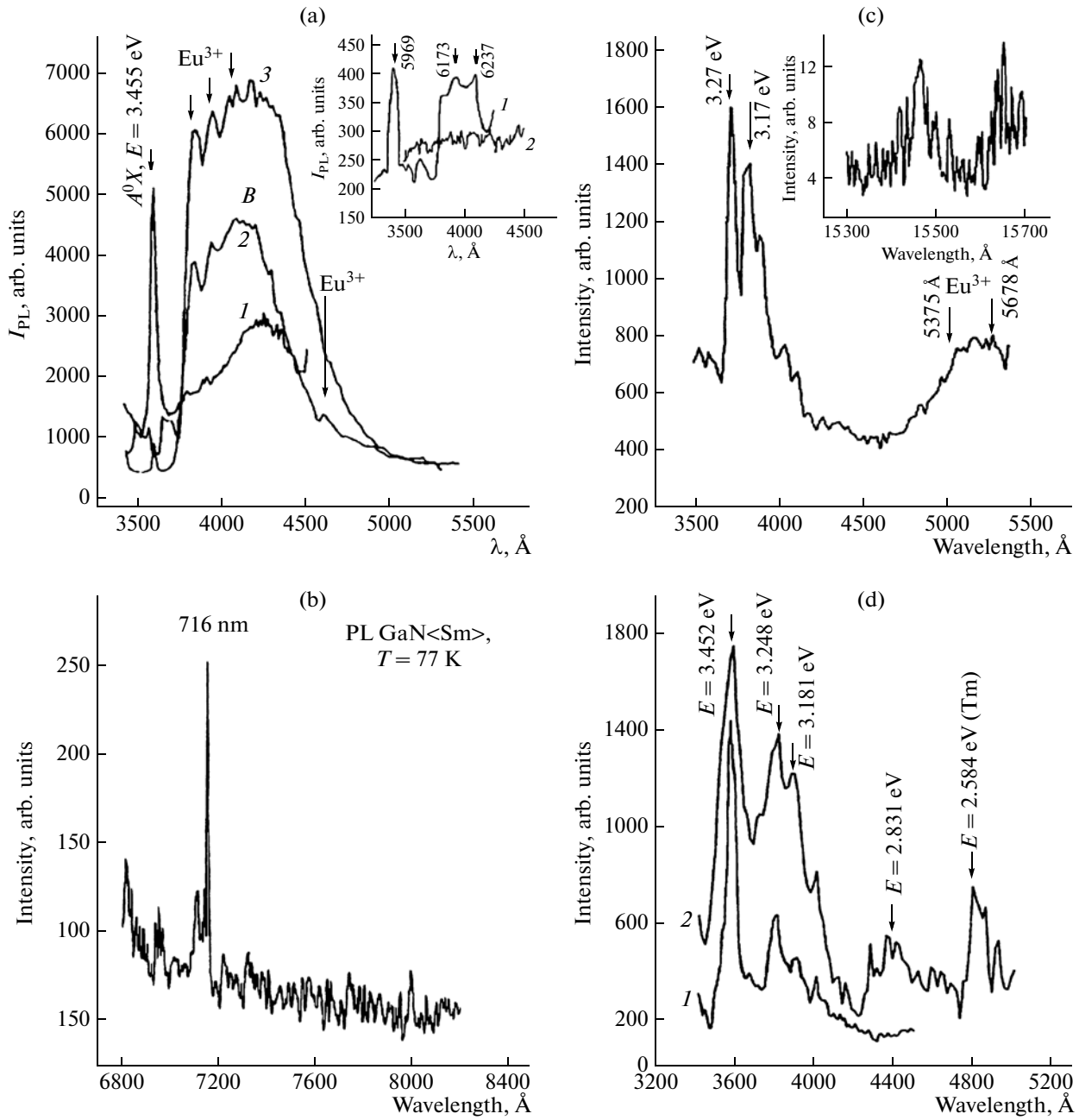

Fig. 3. Spectra of intracenter 4*f* transitions in GaN films, T = 78 K: (a) Eu, (b) Sm, (c) Er, and (d) Tm.

transition from a single-crystal to a polycrystalline structure, which occurs as the Eu content is varied in the range 2–3.5%. The increase in the intensity of the emission line at λ = 622 nm upon a change in the REI content in the range 0.6–1.8% can be due to a rise in the number of emitting centers, and the sharp fall observed as the REI content is increased to within the range 4–8% may be associated with concentration quenching.

Similar results were obtained in [25]. At [Eu] > 2%, concentration quenching of the emission due to intracenter 4*f* transitions in Eu^{3+} was observed. At a content of 16%, RHEED data demonstrated the presence of the EuN phase, which is an indirect-gap semiconductor.

The effect of the defect concentration in the semiconductor matrix on the emission intensity of intracenter transitions was studied on InGaN/GaN structures with multiple QWs (MQWs) doped with Sm, Eu, and Er [26]. At a low defect concentration, there is emission due to intracenter transitions in the REIs, and an increase in the defect concentration causes

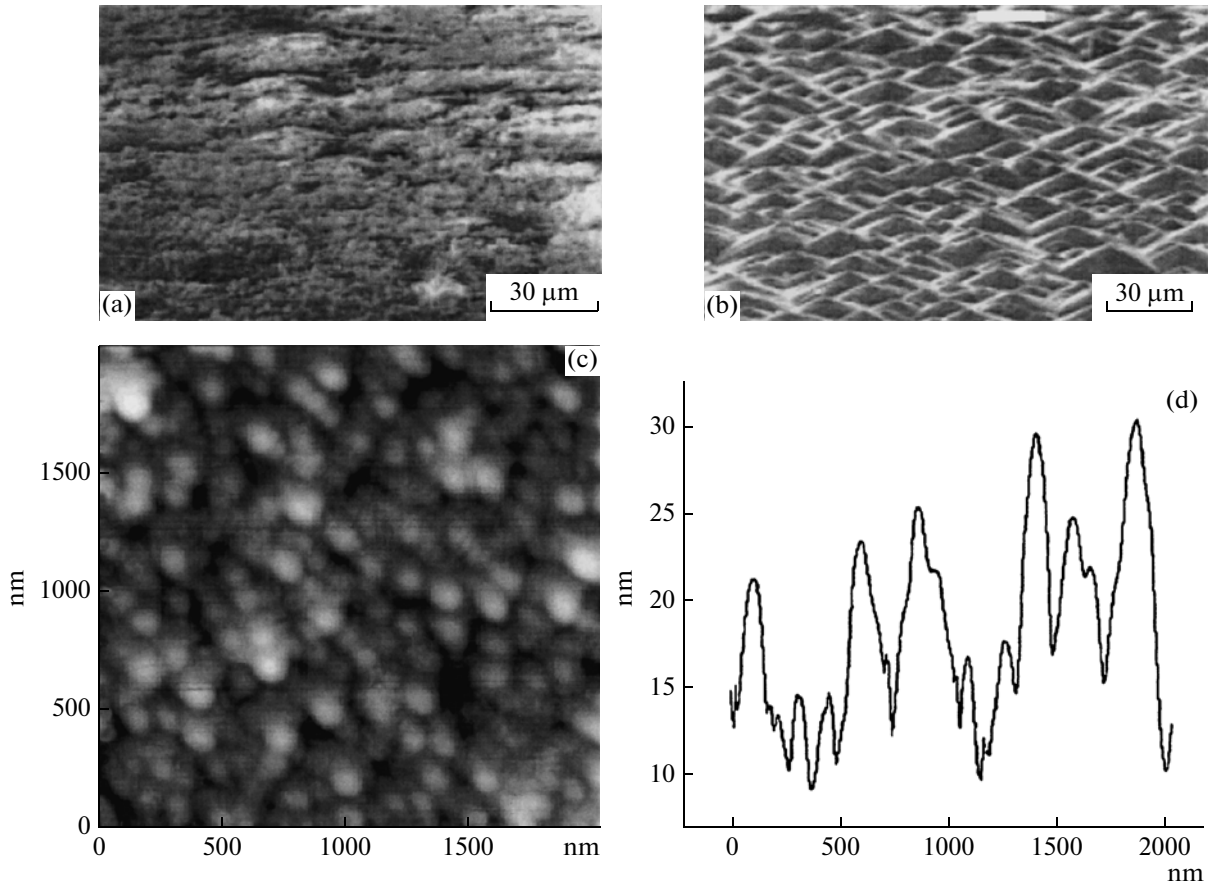

Fig. 4. Surface morphology and the heights of microirregularities of *n*-GaN films: (a, b) electron microscopy data and (c, d) AFM data. $T = 300$ K. (a) *n*-GaN:Eu, (b) *n*-GaN:(Eu + Zn), (c) *n*-GaN:(Mg + Er + Zn); (d) microirregularity heights in a *n*-GaN:(Mg + Er + Zn) film.

defect gettering, as also in the case of crystalline GaN films.

A specific feature of LEDs based on REI-doped GaN (GaN⟨*RE*⟩) is that there is a sharp emission peak (i.e., a peak with a small full width at half maximum, FWHM), which rules out the use of filters. The intensity of emission due to intracenter 4*f* transitions increases with increasing pump current.

The emission spectra of single-crystal ZnO films are similar to the spectra of bulk ZnO crystals [20] and are comparable in emission intensity *I*, FWHM, and peak position λ_{max} of the emission line.

To obtain effective emission from intracenter 4*f* transitions, it is necessary to provide, in addition to the required high concentration of optically active rare-earth ions, effective ways for excitation energy transfer from the matrix to ions and ensure that there is the minimum concentration of impurity–defect complexes. It is known that REIs may possibly occupy the position of an impurity at grain boundaries and inside ZnO grains. It has been suggested [31] that, as a rule, REIs are located on the surface of ZnO crystallites and the emission intensity of intracenter transitions is for the most part determined by the trap concentration V_0. The presence of oxides, REI–O complexes, is a source of emission due to intracenter 4*f* transitions in REIs. At the same time, a low concentration of REI impurities situated on the surface of crystallites results in a low emission intensity due to intracenter 4*f* transitions, as takes place in [30].

The presence of a defect–vacancy of ionized oxygen, V_O, and interstitial Zn atoms makes probable the position of the REI as a substitutional impurity in the form of a REI–V_O complex. Irrespective of the REI's position (at the grain boundary or as a substitutional impurity), its excitation with energy transfer can occur both with and without charge transfer, with various emission intensities. According to [32], the mechanism of excitation with charge transfer is, in all probability, operative because the matrix always has a suitable impurity level that serves as the first stage of energy transfer. The ion (for example Eu) may be present in two different charge states, Eu^{3+} and Eu^{2+}, and energy transfer occurs with charge transfer via a trap level with $E = 3.02$ eV. Despite consideration of the charge-transfer mechanism in the case of doping

with Eu [30], no emission band characteristic of intracenter transitions in Eu^{2+} ($\lambda = 469.7$ nm) is observed and there are emission lines typical of Eu^{3+}.

As for additionally introduced impurities (co-dopants) which promote an increase in the intensity of emission due to intracenter transitions in REIs, it is appropriate to consider the mechanism of impurity interaction, i.e., the kick-out or dissociation mechanism. Changes in the lattice constants upon the introduction of an impurity will govern the influence exerted by the subsequently introduced impurity and, in particular, will determine the solubility limit of the latter in the semiconductor matrix. The influence of REIs as co-dopants was considered in detail for the example of excitation transfer from Yb to Er [32, 33], with a scheme of transitions in various semiconductor matrices considered.

All the PL spectra due to intracenter 4*f* transitions in REIs in single-crystal ZnO films are inhomogeneously broadened. This broadening of the emission line, characterized by the value of the FWHM, arises as the emission wavelengths corresponding to the radiative recombination of carriers localized at different centers are somewhat dissimilar. The reason for this difference is in the spread of the thermal activation energy for the levels, ΔE_{DT}, caused by different values of the local potential V_{loc} at positions associated with REI defects. Consequently, the larger the FWHM of the lines characteristic of intracenter 4*f* transitions, the higher the probability of a different impurity positions in the matrix. Therefore, the form of the PL spectra and, in particular, the FWHM of the emission band associated with intracenter transitions was used to evaluate the probability of various REI positions in doped single-crystal ZnO films. In all probability, the semiconductor matrix of ZnO films on a Si/SiC substrate enables emission sensitization due to intracenter 4*f* transitions in the REIs.

The intensity of the emission due to intracenter 4*f* transitions in REIs introduced into the semiconductor matrix is found to be determined by their local environment as a result of comparing the formation mechanisms for the emission spectra of the intracenter 4*f* transitions in *a*-Si:H amorphous films and in crystalline films of GaN and ZnO doped with REIs. In the case of *a*-Si:H, a pseudo-octahedron with the point group C_{4V} is formed by nanocrystallites, which provides a local environment for the REIs. In the case of the hexagonal crystal lattice in crystalline GaN and ZnO films, the local symmetry of the REIs with a pseudo-octahedron with the point group C_{4V} is created by stresses caused by incorporation of a REI–O complex with a radius exceeding that of the host ions it substitutes.

The mechanism of energy transfer from the semiconductor matrix to the REIs via Auger recombination requires that defects present in the matrix provide the necessary concentration of radiative-recombination centers. ZnO crystals may contain the V_{ZnO-O} defect, a deep acceptor with an emission band at $\lambda = 520–540$ nm, which makes emission due to 4*f* transitions in REIs probable. Oxygen is in the ionized state in ZnO and in the neutral state in GaN; as a consequence of this the probability of the appearance of REI–O complexes in ZnO exceeds that in GaN. If the concentration of the above-mentioned defects is high, the intensity of emission due to intracenter 4*f* transitions is low, as observed previously [30].

In the present study, the diffusion method was used to introduce REIs into the ZnO matrix, which made it possible to bring about minimal changes to the crystal structure of the initial semiconductor matrix. Doping with REIs by the diffusion method was performed on ZnO films produced by the magnetron sputtering of a ZnO target in an Ar + O gas mixture.

The PL spectrum of the initial ZnO films is shown in Fig. 5a. The PL spectrum is broadened in the near-band-edge-photoluminescence (NBEPL) spectral range ($\lambda_{max} = 368$ nm), i.e., the emission peak corresponds to the position of a *B* exciton (D^0, X_B) bound to a neutral donor, FWHM = 37 meV. The PL spectrum has an emission band in the long-wavelength spectral range ($\lambda_{max} = 520–540$ nm), but no emission bands characteristic of the phonon-replica lines of the *B* exciton (D^0, X_B).

According to X-ray diffraction data, the ZnO films under study are single-crystalline with the *Z*(1111) axis perpendicular to the film plane. As indicated by X-ray fluorescence analysis data, the ZnO films under study contain a Fe impurity, which may lead [30, 31] to a decrease in the emission intensity in the NBEPL spectral range, and just this behavior is observed in the given case. At the same time, according to the data of [34] for GaN:(Fe, Eu), the presence of the background Fe impurity may be a cause of sensitization of the emission due to intracenter 4*f* transitions in Eu because of the change in the local environment of the rare-earth ion. Prior to the introduction of REIs, the ZnO films used in our study were annealed in ionized nitrogen in the high-frequency discharge of an Ar + N gas mixture in order to reduce the emission intensity for the band at $\lambda_{max} = 520–540$ nm.

Figure 5b shows how annealing in ionized nitrogen affects the PL spectra of ZnO films at $T = 78$ K and $\lambda = 325$ nm: a 4-nm shift to longer wavelengths is observed ($\lambda_{max} = 372$ nm), which corresponds to the position of an *A* exciton bound to a neutral donor, D^0, X_A; the FWHM decreases to 35 meV, which corresponds to a substantial decrease in the emission intensity in the long-wavelength spectral range, with $\lambda_{max} = 520–540$ nm.

It is assumed that the pronounced changes in the PL spectra of ZnO films as a result of annealing are determined not only by a decrease in the concentration of V_{ZnO-O} defects and by the concentration of

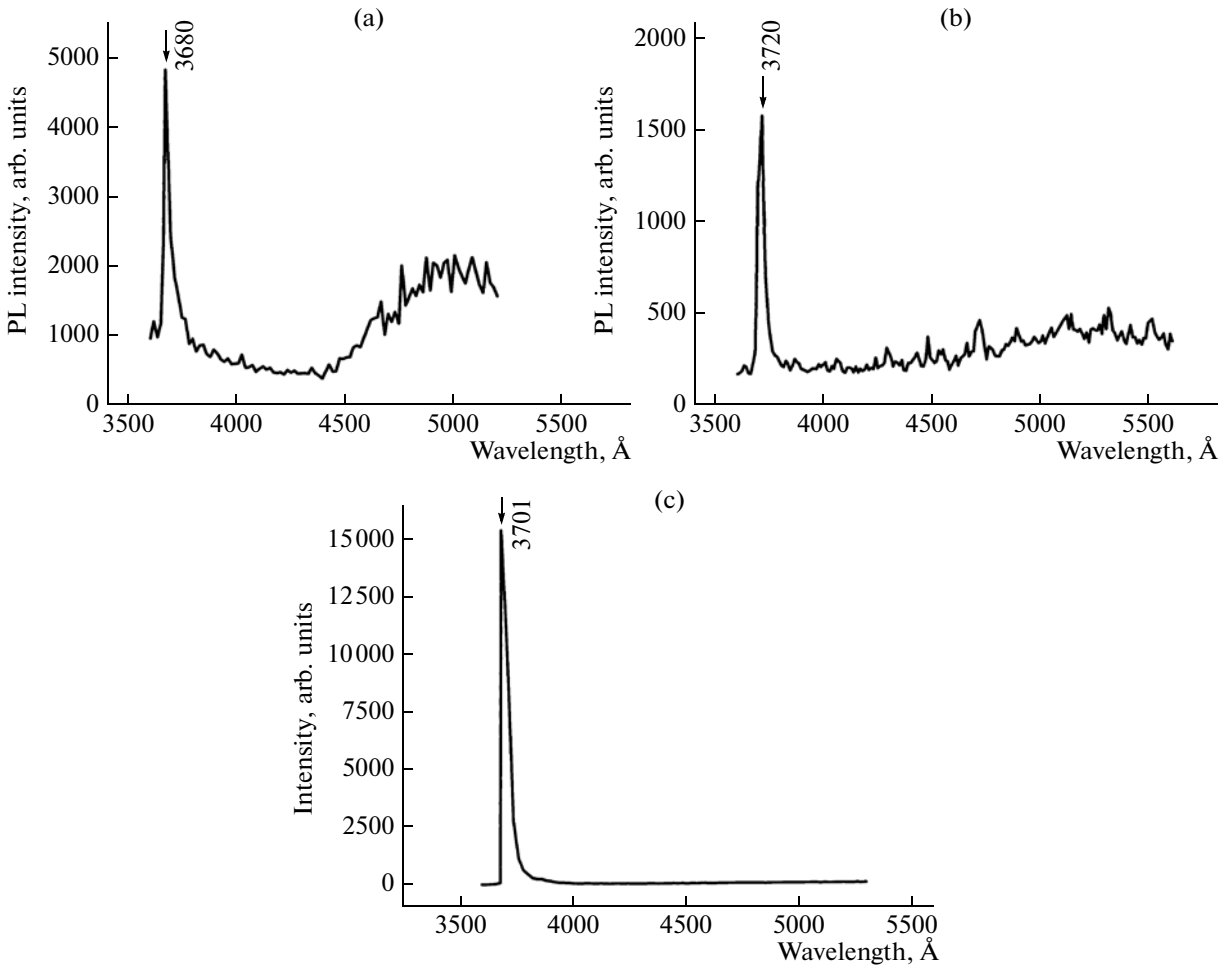

Fig. 5. (a) PL spectrum of an undoped ZnO film, $T = 78$ K. (b) Effect of annealing in ionized nitrogen on the PL spectra of ZnO films, $T = 78$ K. (c) PL spectrum of ZnO films annealed in a nitrogen plasma, $T = 15$ K.

introduced nitrogen, but also by a transformation of the crystal structure and, probably, by a decrease in mismatch stresses, which is indicated by the shift of λ_{max} to longer wavelengths upon annealing. It should be noted that silicon Si with 6*H*-SiC deposited onto it by the method of solid-phase reactions served as substrates for the ZnO films, and it is this that determines the magnitude of the mismatch stresses and, consequently, the shift of λ_{max} to longer wavelengths for ZnO films upon their annealing in ionized nitrogen.

The PL spectrum of ZnO films annealed in a nitrogen plasma, measured at $T = 15$ K, is shown in Fig. 5c. It can be seen that lowering the measurement temperature from $T = 78$ K results in a decrease in λ_{max} to 370.1 nm, and a decrease in the FWHM to 36.9 meV; the emission intensity grows; and there is hardly any emission with $\lambda_{max} = 520$–540 nm in the long-wavelength range of the spectrum.

Figure 6 shows the PL spectra of ZnO films doped with Eu (Fig. 6a), Er (Fig. 6b), Sm (Fig. 6d), Yb (Fig. 6e), and Tm (Fig. 6c). Figure 6a presents the PL spectra of films doped with Eu ($T = 78$ K, $\lambda = 325$ nm). The PL is shown for the spectral range characteristic of 4*f* transitions in Eu; the FWHM = 42 meV for $\lambda = 590$ nm $^5D_0$–$^7F_1$ transitions and the FWHM = 38 meV for the emission line with $\lambda = 623$ nm for the $^5D_1$–$^7F_1$ transition.

Figure 6b shows the PL spectrum for Er-doped ZnO films in the short- and long-wavelength spectral regions.

In the IR spectral range, an emission band can be seen at $\lambda = 1530$ nm (FWHM = 10 meV). This band, characteristic of intracenter 4*f* transitions in Er ($^4I_{15/2}$–$^4I_{13/2}$), is only observed upon the additional introduction of a Ce co-dopant and also under additional excitation with an Ar laser ($\lambda = 488$ nm).

The intensity of emission due to intracenter 4*f* transitions in REIs (Eu, Er) is low in the case of the doping of ZnO films with a single impurity, which may be due to both a low concentration of dopants (Figs. 6a and 6b) and to segregation of the Eu and Er impurities, which leads to a nonoptimal local crystalline (ligand)

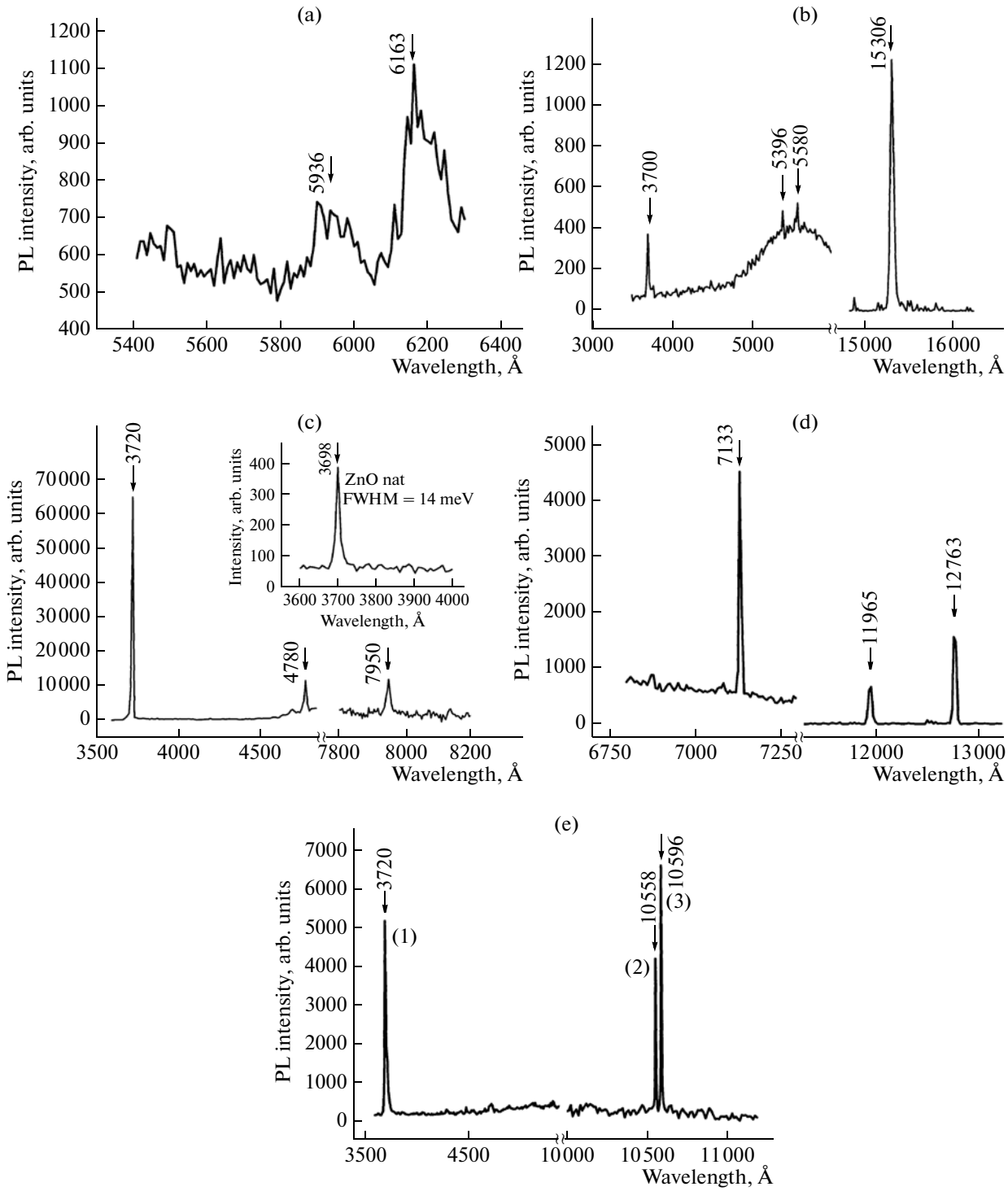

Fig. 6. Effect of doping with REIs on the PL spectra of ZnO films, $T = 78$ K: (a) Eu; (b) Er; (c) Tm; the inset: spectrum of an undoped ZnO film in the NBEPL spectral range; (d) Sm; and (e) Yb.

environment. Previously, low-intensity emission lines characteristic of intracenter transitions in Er were also observed in [30], but the ZnO films were not subjected to post-growth treatment in the high-frequency discharge of an Ar + N gas mixture. Moreover, the concentration ($C_{Er} < 10^{17}$ cm^{-3}) was insufficient for obtaining the high-intensity emission characteristic of intracenter 4*f* transitions in Er.

Compared with the intensity of emission due to intracenter transitions in Eu and Er, the intensity of intracenter transitions in Sm and Tm in ZnO films is rather high (Figs. 6c, 6d). Previously, it has been

shown for the example of wurtzite *n*-GaN crystals doped with Sm or Tm that the intensity of the emission characteristic of intracenter 4*f* transitions in these REIs exceeds that for Er and Eu at the same concentration of introduced impurities. The increase in emission intensity was attributed to the low segregation capacity of Sm and Tm [13].

In the visible spectral range, the PL spectrum of ZnO films doped with Sm or Tm shows a significant increase in the emission intensity in the NBEPL spectral range, compared with that of an undoped film, i.e., the gettering effect is observed. In addition, the FWHM decreases, which, together with the increase in the intensity of the emission from ZnO films in the NBEPL spectral range as a result of doping with Sm or Tm, may enable lasing.

Figure 6c shows the PL spectrum of a Tm-doped ZnO film in the visible spectral range. An emission band in the NBEPL spectral range and an emission band at $\lambda = 478$ nm (FWHM = 11 meV), characteristic of intracenter 4*f* transitions in Tm ($^1G_4$–$^3H_6$ transition), can be seen. The inset in Fig. 6c shows the PL spectrum of an undoped ZnO film (FWHM = 40 meV), whose emission intensity in the NBEPL spectral range is low. As a result of doping with Tm, the FWHM in the NBEPL spectral range became 16 meV and the emission intensity increased by more than two orders of magnitude (by a factor of 150), which is indicative of REI defect gettering in the semiconductor matrix [15]. The position of $\lambda_{max} = 372$ nm remained the same as that in the undoped ZnO film.

Figure 6d shows the PL spectrum of Sm-doped ZnO films in the visible spectral region.

In the visible spectral range, the intensity of emission due to intracenter 4*f* transitions in Sm (Fig. 6d) at $\lambda = 713.3$ nm (FWHM = 4.5 meV) indicates, as also in the case of *n*-GaN [13], that the concentration of optically active impurity ions is high and the local environment of the Sm^{3+} ion is optimal. The long-wavelength region of the spectrum in Fig. 6d illustrates the effect of additional excitation on the intensity of emission due to 4*f* transitions in Sm in the near-IR spectral range ($\lambda = 1195$ and 1276 nm), for which the FWHM = 3.14 meV.

It has been shown previously that the intensity of emission due to intracenter 4*f* transitions in Sm introduced into InGaN/GaN QW structures is insignificant. The dopant was situated in the *n*-GaN barrier layer [14], which suggests a rather high concentration of defects in the barrier layer of the structures. Thus, with an REI introduced as an optical probe, it is possible to make a judgment about the parameters of the semiconductor matrix on the basis of the intensities of emission due to intracenter 4*f* transitions.

Figure 6e shows the effect of another REI activator, Er, on the PL spectrum of a ZnO film doped with Er + Yb; in the near-IR spectral range $\lambda = 1059.4$ nm (FWHM = 1.2 meV) and there is a band at 1055.8 nm (FWHM = 1.2 meV).

4. CONCLUSIONS

It was shown by comparing the formation mechanisms of the emission spectra of intracenter 4*f* transitions in REI-doped amorphous *a*-Si:H films and in crystalline GaN and ZnO films that the intensity of emission due to intracenter 4*f* transitions is determined by the local environment of REIs in the semiconductor matrix. In the case of *a*-Si:H, a pseudo-octahedron with the point group C_{4V} is formed by REI–O nanocrystallites. In the case of the hexagonal lattice in crystalline GaN and ZnO films, the local symmetry of REIs with a pseudo-octahedron with the point group C_{4V} is due to stresses caused by the incorporation of a REI–O complex with a larger radius, compared with the host ions being substituted, at crystal lattice sites. The mechanism of Auger recombination and excitation transfer from the semiconductor matrix to the REIs requires that the matrix contain defects providing the necessary concentration of radiative-recombination centers. It is assumed that the role of defects of this kind in crystalline GaN and ZnO films is played by defects present in the optimal concentration, which are responsible for the appearance of the emission band at $\lambda = 520$–540 nm and are associated with the presence of oxygen, i.e., the same mechanism as that in *a*-Si:H films is operative here.

It should also be taken into account that ZnO films exhibit, in contrast to GaN films, high-intensity emission in the long-wavelength spectral region, characteristic of intracenter transitions in REIs, and a significant increase in the emission intensity in the short-wavelength spectral range ($\lambda = 368$–370 nm) on being doped with Tm, Sm, or Yb. REI-doped GaN films have only an inhomogeneously broadened emission spectrum in this spectral range due to the presence of an emission band characteristic of donor–acceptor recombination.

High-intensity emission with small FWHM in various spectral ranges makes ZnO a promising material for optoelectronic devices operating not only in the IR, but also in the UV spectral range.

ACKNOWLEDGMENTS

The study was supported by the Program of the Presidium of the Russian Academy of Sciences "Strongly correlated systems."

The authors are grateful to N.N. Syrnikova for X-ray diffraction analyses of ZnO films.

REFERENCES

1. J. H. Park and A. J. Steckel, Appl. Phys. Lett. **85**, 4588 (2004).

2. Y. Fujywara, A. Nishikawa, and Y. Terray, in *Proceedings of the Advanced Display Technologies International Symposium, St.-Petersburg State Technol.-Tech. University, Sept. 27–Oct. 1, 2010* (St.-Petersburg, 2010), p. 210.
3. M. Zamfierscu, A. Kavokin, B. Gil, G. Malpuech, and M. Kaliteevski, Phys. Rev. B **65**, 165205 (2002).
4. M. K. Chong, A. P. Abiyassa, K. Pita, and S. F. Yu, Appl. Phys. Lett. **95**, 151105 (2008).
5. Y. Liu, Ch. Xu, and Q. Jang, J. Appl. Phys. **105**, 084701 (2009).
6. V. F. Masterov, F. S. Nasredinov, P. P. Seregin, E. I. Terukov, and M. M. Mezdrogina, Semiconductors **32**, 636 (1998).
7. M. M. Mezdrogina, M. P. Annaorazova, E. I. Terukov, I. N. Trapeznikova, and N. Nazarov, Semiconductors **33**, 1145 (1999).
8. M. M. Mezdrogina, G. N. Mosina, E. I. Terukov, and I. N. Trapeznikova, Semiconductors **35**, 684 (2001).
9. Zh. Ataev, V. A. Vasiliev, I. A. Elizarov, and M. M. Mezdrogina, Semiconductors **29**, 799 (1995).
10. P. H. Citrin, P. A. Northrup, R. Birkhahn, and A. J. Steckel, Appl. Phys. Lett. **78**, 2865 (2000).
11. Yu. V. Zhilyaev, V. V. Krivolapchuk, M. M. Mezdrogina, S. D. Raevskii, and Sh. A. Yusupova, in *Proceedings of the International Conference on Photoluminescence and Electroluminescence in Semiconductors and Insulators* (St.-Petersburg, 2001), p. 21.
12. T. Andreev, N. Q. Liem, Y. Hori, M. Tanaka, O. Oda, D. L. S. Dang, and B. Daulnet, Phys. Rev. B **73**, 195203 (2006).
13. M. M. Mezdrogina, E. Yu. Danilovskii, and R. V. Kuzmin, Inorg. Mater. **47**, 1450 (2011).
14. J.-S. Filhol, R. Jones, M. J. Shaw, and P. R. Briddon, Appl. Phys. Lett. **84**, 2841 (2004).
15. H. J. Lozykowski, Phys. Rev. B **48**, 17758 (1993).
16. V. V. Krivolapchuk and M. M. Mezdrogina, Phys. Solid State **46**, 2201 (2004).
17. S. O. Kucheyev, J. E. Bradly, S. Ruffelt, C. P. Li, T. E. Felter, and A. V. Hamza, Appl. Phys. Lett. **90**, 221901 (2007).
18. M. M. Mezdrogina and V. V. Krivolapchuk, Phys. Solid State **48**, 1250 (2006).
19. M. M. Mezdrogina, V. V. Krivolapchuk, V. N. Petrov, S. N. Rodin, and A. V. Chernyakov, Semiconductors **40**, 1378 (2006).
20. P. D. Dapkus, W. H. Hackett, Jr., O. G. Lorimor, and R. Z. Bachrach, J. Appl. Phys. **45**, 4290 (1974).
21. H. W. Moos, J. Luminesc. **1–2**, 106 (1970).
22. B. A. Wilson, W. M. Yen, J. Hagarty, and G. F. Imbusch, Phys. Rev. B **19**, 4238 (1979).
23. H. Wu, C. B. Poitras, M. Lipson, M. G. Spenser, J. Hunting, and F. J. DiSalvo, Appl. Phys. Lett. **88**, 011921 (2006).
24. R. Wang, A. J. Steckel, E. E. Brown, U. Hommerlich, and J. Zavada, J. Appl. Phys. **105**, 043107 (2009).
25. H. Bang, S. Morishima, J. Sawahata, J. Seo, M. Takigushi, M. Tsunemi, K. Okamoto, and M. Nomura, Appl. Phys. Lett. **85**, 227 (2004).
26. M. M. Mezdrogina, V. V. Krivolapchuk, V. N. Petrov, Yu. V. Kozhanova, E. Yu. Danilovskii, and R. V. Kuz'min, Semiconductors **43**, 447 (2009).
27. R. Birkahn, M. Garter, and A. J. Steckel, Appl. Phys. Lett. **74**, 2161 (1999).
28. L. Huang, J. Labis, and S. C. Ray, Appl. Phys. Lett. **96**, 062112 (2010).
29. Zh. Zhou and N. Matsunami, Appl. Phys. Lett. **86**, 041107 (2005).
30. M. Mezdrogina, V. V. Krivolapchuk, N. A. Feoktistov, E. Yu. Danilovskii, R. V. Kuz'min, S. V. Razumov, S. A. Kukushkin, and A. V. Ospiov, Semiconductors **42**, 766 (2008).
31. M. M. Mezdrogina, M. V. Eremenko, S. M. Golubenko, and S. V. Razumov, Fiz. Tverd. Tela **54** (6) (2012, in press).
32. Y. Liu, Ch. Xu, and Q. Yang, J. Appl. Phys. **104**, 064701 (2008).
33. A. S. S. de Camargo, E. R. Botero, E. R. M. Andreeta, D. Garcia, J. A. Eiras, and L. A. O. Nunes, Appl. Phys. Lett. **86**, 241112 (2005).
34. M. M. Mezdrogina, E. Yu. Danilovskii, and R. V. Kuz'min, Semiconductors **44**, 321 (2010).

Translated by M. Tagirdzhanov